An H∞-based approach for robust sensor localization

Usman A. Khan, Anton Korniienko, Karl Henrik Johansson

An H_∞-based approach for robust sensor localization

Usman A. Khan, Anton Korniienko, and Karl H. Johansson

***Abstract*— In this paper, we consider the problem of sensor localization, i.e., finding the positions of an arbitrary number of sensors located in a Euclidean space, $\mathbb{R}^m$, given at least $m+1$ anchors with known locations. Assuming that each sensor knows pairwise distances in its neighborhood and that the sensors lie in the convex hull of the anchors, we provide a DIstributed LOCalization algorithm in Continuous-Time, named *DILOC-CT*, that converges to the sensor locations. This representation is linear and is further decoupled in the coordinates.**

By adding a proportional controller in the feed-forward loop of each location estimator, we show that the convergence speed of DILOC-CT can be made arbitrarily fast. Since a large gain may result into unwanted transients especially in the presence of disturbance introduced, e.g., by communication noise in the network, we use H_∞ theory to design local controllers that guarantee certain global performance while maintaining the desired steady-state. Simulations are provided to illustrate the concepts described in this paper.

I. Introduction

Localization is often referred to as finding the position of a point in a Euclidean space, $\mathbb{R}^m$, given a certain number of *anchors*, with perfectly known positions, and point-to-anchor distances and/or angles. Traditionally, distance-based localization has been referred to as *trilateration*, whereas angle-based methods are referred to as *triangulation*. Trilateration is the process of finding a location in $\mathbb{R}^m$, given only the distance measurements to at least $m+1$ anchors, see Fig. 1 (Left). With $m+1$ sensor-to-anchor distances, the *nonlinear* trilateration problem is to find the intersection of three circles. Triangulation, Fig. 1 (Right), employs the angular information to find the unknown location.

The literature on localization is largely based on the triangulation and trilateration principles, or in some cases, a combination of both. Recent work may be broadly characterized into centralized and distributed algorithms, see [1] where a comprehensive coverage of cooperative and non-cooperative strategies is provided. Centralized localization algorithms include: maximum likelihood estimators, [2], [3]; multi-dimensional scaling (MDS), [4], [5]; optimization-based methods to include imprecise distance information, see [6]; for additional work, see [7]–[9]. Optimization based techniques can be found in [10], [11] and references therein, whereas, polynomial methods are described in [12].

UAK is with the Department of Electrical and Computer Engineering at Tufts University, Medford, MA 02155, USA, khan@ece.tufts.edu. His work is supported by an NSF Career award # CCF-1350264.

AK is with Laboratoire Ampère, École Centrale de Lyon, 69134 Ecully Cedex, France, anton.korniienko@ec-lyon.fr. His work is supported by a grant from la Région Rhône-Alpes.

KHJ is with the KTH ACCESS Linnaeus Center, School of Electrical Engineering, Royal Institute of Technology (KTH), Stockholm, Sweden, kallej@ee.kth.se. His work is supported by the Knut and Alice Wallenberg Foundation and the Swedish Research Council.

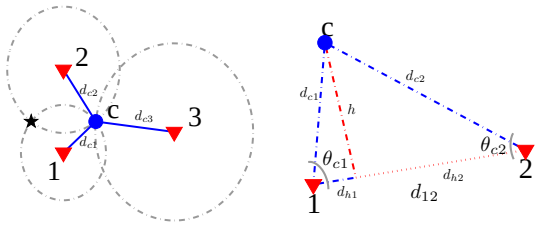

Fig. 1. Localization in $\mathbb{R}^2$, anchors: red triangles; unknown location: blue circle. (Left) *Trilateration*–the unknown location is at the intersection of three circles. (Right) *Triangulation*–the line segments, $h, d_{c1}, d_{c2}, d_{h1}$, and d_{h2}, are computed from trigonometric operations.

Distributed localization algorithms can be characterized into two classes: multilateration and successive refinements. In *multilateration algorithms*, [13], [14], each sensor estimates its distance from the anchors and then calculates its location via trilateration; multilateration implies that the distance computation may require a multi-hop communication. Distributed multidimensional scaling is presented in [15]. *Successive refinement algorithms* that perform an iterative minimization of a cost function are presented in, e.g., [16], which discusses an iterative scheme where they assume 5% of the nodes as anchors. Reference [17] discusses a Self-Positioning Algorithm (SPA) that provides a GPS-free positioning and builds a relative coordinate system. Other related work also consists of graph-theoretic approaches [18], [19], and probabilistic methods, [20], [21].

Of significant relevance to this paper is Ref. [22], which describes a discrete-time algorithm, named *DILOC*, assuming a *global convexity* condition, i.e., each sensor lies in the convex hull of at least $m+1$ anchors in $\mathbb{R}^m$. A sensor may find its location as a linear-convex combination of the anchors, where the coefficients are the barycentric coordinates; attributed to August F. Möbius, [23]. However, this representation may not be practical as it requires long-distance communication to the anchors. To overcome this issue, each sensor finds $m+1$ neighbors, its triangulation set, such that it lies in their convex hull and iterates on its location as a barycentric-based representation of only the neighbors. Assuming that each sensor can find a triangulation set, DILOC converges to the true sensor locations. Ref. [22] analyzes the convergence and provides tests for finding triangulation sets with high probability in a small radius.

In this paper, we provide a continuous-time analog of DILOC-DT in [22], that we call *DILOC-CT*, and show that by using a proportional controller in each sensor's location estimator, the convergence speed can be increased arbitrarily. Since this increase may come at the price of unwanted

transients especially when there is disturbance introduced by the network, we replace the proportional gain with a dynamic controller that guarantees certain performance objectives. We thus consider disturbance in the communication network that is incurred as zero-mean additive noise in the information exchange. In this context, we study the disturbance rejection properties of the local controllers and tune them to withstand the disturbance while ensuring some performance objectives. Our approach is based on H_∞ design principles and uses the input-output approach, see e.g., [24]–[27].

Notation: The superscript, 'T', denotes a real matrix transpose while the superscript, '$*$', denotes the complex-conjugate transpose. The $N \times N$ identity matrix is denoted by I_N and the $n \times m$ zero matrix is denoted by $0_{n\times m}$. The dimension of the identity or zero matrix is omitted when it is clear from the context. The diagonal aggregation of two matrices A and B is denoted by $\text{diag}(A, B)$. The *Kronecker product*, denoted by $\otimes$, between two matrices, A and B, is defined as $A \otimes B = [a_{ij}B]$. We use $T_{x\to y}(s)$ to denote the transfer function between an input, $x(t)$, and an output, $y(t)$. With matrix, G, partitioned into four blocks, $G_{11}, G_{12}, G_{21}, G_{22}$, $G \star K$ denotes the *Redheffer* product, [31], i.e.,

$$G \star K = G_{11} + G_{12}K\left(I - G_{22}K\right)^{-1} G_{21}.$$

Similarly, $K \star G = G_{22} + G_{21}K\left(I - G_{11}K\right)^{-1} G_{12}$. For a stable LTI system, G, $\|G\|_\infty$ denotes the H_∞ norm of G. For a complex matrix, P: $\bar{\sigma}(P)$ denotes its maximal singular; $\lambda_i(P)$ denotes the ith eigenvalue; and $\rho(P)$ denotes its spectral radius. Finally, the symbols, '$\geq$' and '$>$, denote positive semi-definiteness and positive-definiteness of a matrix, respectively.

We now describe the rest of the paper. Section II describes the problem, recaps DILOC-DT, and introduces the continuous-time analog, DILOC-CT. Section III derives the convergence of DILOC-CT with a proportional gain and investigates disturbance-rejection. In Section IV, we describe dynamic controller design using the H_∞ theory according to certain objectives that ensure disturbance rejection. Section V illustrates the concepts and Section VI concludes the paper.

II. Preliminaries and Problem Formulation

Consider a network of M sensors, in the index set Ω, with unknown locations, and N anchors, in the index set κ, with known locations, all located in $\mathbb{R}^m$, $m \geq 1$; let $\Theta = \Omega \cup \kappa$ be the set of all nodes. Let $\mathbf{x}^{i*} \in \mathbb{R}^m$ denote the *true location* of the ith sensor, $i \in \Omega$; similarly, $\mathbf{u}^j \in \mathbb{R}^m, j \in \kappa$, is the true location of the anchors. We assume that each sensor is able to compute its distances to the nearby nodes (sensors and/or anchors) by using, e.g., the Received Signal Strength (RSS) or camera-based methods, [2], [28]. The problem is to find the locations of the sensors in Ω. Below, we describe DILOC, which was originally introduced in [22].

A. DILOC-DT

DILOC-DT assumes that each sensor lies in the convex hull, denoted by $\mathcal{C}(\kappa)$, of the anchors. Using only the inter-node distances, each sensor, say i, finds a *triangulation set*, Θ_i, of $m+1$ neighbors such that $i \in \mathcal{C}(\Theta_i), |\Theta_i| = m+1$. A convex hull inclusion test is given by

$$i \in \mathcal{C}(\Theta_i), \qquad \text{if } \sum_{j\in\Theta_i} A_{\Theta_i\cup\{i\}\setminus j} = A_{\Theta_i},$$

where A_{Θ_i} denotes the m-dimensional volume, area in $\mathbb{R}^2$ or volume in $\mathbb{R}^3$, of $\mathcal{C}(\Theta_i)$, see Fig. 2 in $\mathbb{R}^2$, and can be computed by Cayley-Menger determinant, [22], [29], using only the pairwise distances of the nodes in $\{i, \Theta_i\}$.

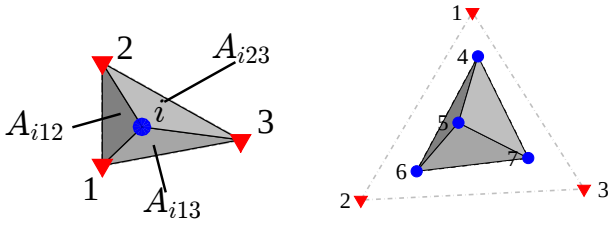

Fig. 2. $\mathbb{R}^2$: (Left) Agent i lies in the convex hull of three anchors. (Right) Sensor 4, 6 and 7 form a triangulation set for sensor 5. Blue circles and red triangles indicate agents and anchors, respectively.

Given a triangulation set, Θ_i, for every $i \in \Omega$, each sensor updates its location estimate, $\mathbf{x}_k^i$, as follows:

$$\mathbf{x}_{k+1}^i = \sum_{j\in\Theta_i\cap\Omega} \underbrace{\frac{A_{\Theta_i\cup\{i\}\setminus j}}{A_{\Theta_i}}}_{\triangleq p_{ij}} \mathbf{x}_k^j + \sum_{j\in\Theta_i\cap\kappa} \underbrace{\frac{A_{\Theta_i\cup\{i\}\setminus j}}{A_{\Theta_i}}}_{\triangleq b_{ij}} \mathbf{u}^j, \quad (1)$$

where k is discrete-time, the coefficients, p_{ij}'s and b_{ij}'s, are the *barycentric coordinates* that are positive and sum to 1. Let $\mathbf{x}_k \in \mathbb{R}^{M\times m}$ be the vector of location estimates, $\mathbf{x}_k^i, i \in \Omega$; similarly, $\mathbf{u}$ for anchors; DILOC-DT is given by

$$\mathbf{x}_{k+1} = P\mathbf{x}_k + B\mathbf{u}, \quad (2)$$

where $P = \{p_{ij}\}$ is an $M \times M$ matrix of the sensor-to-sensor barycentric coordinates; similarly, $B = \{b_{ij}\}$ is $M \times N$. The following result is from [22].

Lemma 1: Let $|\kappa| \geq m+1$ and $i \in \mathcal{C}(\kappa), \forall i \in \Omega$. Assume non-trivial configurations, i.e., $A_\kappa \neq 0, A_{\Theta_i} \neq 0, \forall i \in \Omega$. Then, DILOC-DT, Eq. (2), is such that $\rho(P) < 1$ and

$$\lim_{k\to\infty} \mathbf{x}_k = (I - P)^{-1}B\mathbf{u} = \mathbf{x}^*, \quad (3)$$

where $\mathbf{x}^*$ is the vector of true sensor locations.

Clearly, the proof relies on the fact that $\rho(P) < 1$, which can be shown with the help of an absorbing Markov chain analogy[1], see [22]. In particular, each transient state (sensor) has a path (possibly over multiple links) to each absorbing state (anchor); subsequently, the (transient) state-transition matrix, P, is such that $\rho(P) < 1$. That $(I - P)^{-1}B\mathbf{u}$ is the desired steady-state can be verified as the true sensor locations follow: $\mathbf{x}^* = P\mathbf{x}^* + B\mathbf{u}$.

[1]Refs. [22], [30] further characterize the probability of successful triangulation, imperfect communication, and noise on the distance measurements, among many other refinements.

B. DILOC-CT

We now provide DILOC-CT, a continuous-time analog to DILOC-DT. To this aim, let $\mathbf{x}_i(t)$ denote the m-dimensional row-vector of sensor i's location estimate, where $t \geq 0$ is the continuous-time variable. Since the anchors' locations are known, we have $\mathbf{u}_j(t) = \mathbf{u}_j, \forall t \geq 0, j \in \kappa$. Borrowing notation from Section II-A, DILOC-CT is given by, where (t) is dropped in the sequel for convenience:

$$\dot{\mathbf{x}}_i = -\mathbf{x}_i + \mathbf{r}_i; \qquad \mathbf{r}_i \triangleq \sum_{j \in \Theta_i \cap \Omega} p_{ij}\mathbf{x}_j + \sum_{j \in \Theta_i \cap \kappa} b_{ij}\mathbf{u}_j, \quad (4)$$

and Θ_i is the triangulation set at sensor i. Note that Θ_i may not contain any anchor, in which case $|\Theta_i \cap \Omega| = m+1$, and $|\Theta_i \cap \kappa| = 0$. In other words, a sensor may not have any anchor as a neighbor and the barycentric coordinates are assigned to the neighboring sensors, with unknown locations.

In order to improve the convergence rate, we may add a proportional gain, $\alpha \in \mathbb{R}$, in the feed-forward loop of each sensor's location estimator, denoted by an identical system, T_s, at each sensor:

$$T_s: \qquad \dot{\mathbf{x}}_i = \alpha(-\mathbf{x}_i + \mathbf{r}_i). \quad (5)$$

We now assume that the received signal at each sensor incurs a zero-mean additive disturbance, $\mathbf{z}_i(t)$, whose frequency spectrum lies in the interval, $[\omega_z^-, \omega_z^+]$. With this disturbance, the location estimator is given by

$$\dot{\mathbf{x}}_i = \alpha(-\mathbf{x}_i + \mathbf{r}_i + \mathbf{z}_i). \quad (6)$$

Here, $\mathbf{z}_i(t)$ can be thought of as communication noise that effects the information exchange. Note that Eq. (4) is special case of Eq. (6) with $\alpha = 1$ and $\mathbf{z} = \mathbf{0}$. Finally, we replace the proportional gain, α, with a local controller, $K(s)$. The overall architecture is depicted in Fig. 3, where we separate the desired signal, $\mathbf{r}_i$, and the disturbance, $\mathbf{z}_i$, as two distinct inputs to each T_s.

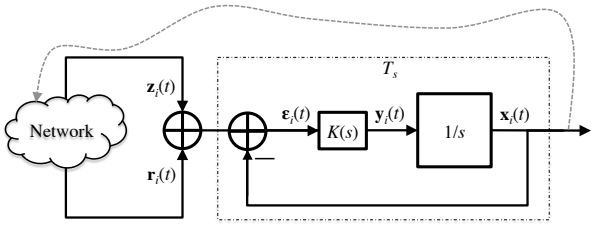

Fig. 3. DILOC-CT architecture

The contributions of this paper are as follows: *First*, we show that DILOC-CT converges to the true sensor locations and characterize the range of gains that ensures this convergence. We then study the disturbance rejection properties of the proportional gain. This analysis is provided in Section III. *Second*, we note that an arbitrary high proportional gain may result in unwanted transients and disturbance amplification. In order to add design flexibility and guarantee certain performance objectives, we replace the proportional gain, α, with local controllers, $K(s)$. We use H_∞ design procedure to derive these local controllers meeting global objectives. This analysis is carried out in Section IV. *Finally*, we study the disturbance rejection properties of the local controllers with the help of the H_∞ design in Sections IV and V.

III. DILOC-CT WITH PROPORTIONAL GAIN

We now analyze the convergence properties of the proportional gain controller without disturbance in Eq. (5). Let $\mathbf{x}(t)$ collect the location estimates at the sensors and let $\mathbf{u}$ collect the true locations of the anchors. Borrowing notation from Section II-A, we use the matrices, P and B, to denote the corresponding barycentric coordinates. Eq. (5) can be equivalently written in the following matrix form:

$$\dot{\mathbf{x}} = -\alpha(I-P)\mathbf{x} + \alpha B\mathbf{u} \triangleq P_\alpha \mathbf{x} + B_\alpha \mathbf{u}. \quad (7)$$

We have the following result.

Lemma 2: If $\rho(P) < 1$, then $\Re\{\lambda_i(P_\alpha)\} < 0, \forall i, \alpha > 0$.

Proof: Let $\lambda_i(P) = a_i + \sqrt{-1}b_i$ for some $a_i, b_i \in \mathbb{R}$, and note that $|a_i| < 1, \forall i$, since $\rho(P) < 1$, then

$$\lambda_i(I-P) = 1 - a_i - \sqrt{-1}b_i, \quad (8)$$

and the lemma follows for any $\alpha > 0$. ■

The following theorem studies the DILOC-CT convergence.

Theorem 1: DILOC-CT, Eq. (7), converges to the true sensor locations, $\mathbf{x}^*$, for all $\alpha > 0$, i.e.,

$$\lim_{t\to\infty} \mathbf{x}(t) = (I-P)^{-1}B\mathbf{u} = \mathbf{x}^*. \quad (9)$$

Proof: From Lemma 2, we have $\Re\{\lambda_i(P_\alpha)\} < 0, \forall i$. Starting from Eq. (7), we get

$$\begin{aligned} \mathbf{x}(t) &= e^{P_\alpha t}\mathbf{x}(0) + \int_0^t e^{P_\alpha \tau}\alpha B\mathbf{u}(t-\tau)d\tau, \\ &= e^{P_\alpha t}\mathbf{x}(0) + P_\alpha^{-1}\left(e^{P_\alpha t} - I\right)\alpha B\mathbf{u}, \end{aligned}$$

which asymptotically goes to (since $\lim_{t\to\infty} e^{P_\alpha t} = \mathbf{0}$)

$$\lim_{t\to\infty} \mathbf{x}(t) = -P_\alpha^{-1}\alpha B\mathbf{u} = -(-\alpha(I-P))^{-1}\alpha B\mathbf{u},$$

and the theorem follows. ■

That the convergence speed is exponential in $\alpha > 0$ can also be easily verified. In fact, the real part of the eigenvalues of P_α move further into the left-half plane as α increases. However, in the presence of network-based disturbances, $\mathbf{z}_i(t)$'s, an arbitrarily large α also amplifies the disturbance. To guarantee certain performance objectives, a natural extension is to replace the proportional (static) gain with a dynamic controller, $K(s)$. We study this scenario using H_∞ design in Section IV.

In the following, we analyze the disturbance rejection with the proportional controller. To proceed, we use the fact that DILOC-CT is decoupled in the coordinates. Hence, each local system, T_s, see Eq. (5) and Fig. 3, can be analyzed per coordinate and the same analysis can be extended to other coordinates. Recall that the network location estimate, $\mathbf{x}(t)$, is a $M \times m$ matrix where each column is associated to a location coordinate in $\mathbb{R}^m$. We let x to be an arbitrarily chosen column of $\mathbf{x}$ corresponding to one chosen dimension. Similarly, we let z, r, ε, and y (signals in Fig. 3) to represent M-dimensional vectors; for any of such vectors, the subscript i denotes the chosen coordinate at sensor i.

A. Rejection vs. Localization tradeoff, $M = 1$

We first consider the simplest case of DILOC-CT in $\mathbb{R}^2$, with static controller, $K(s) = \alpha$, $N = 3$ anchors and one sensor, $M = 1$, see Fig. 2 (Left). In this case, the dynamics of the overall network is equivalent to the dynamics, T_s in Eq. (5), of one sensor and a constant input r_i defined by Eq. (4) with $p_{ij} = 0$. Since the H_∞ design approach used in the next sections is frequency-based, the localization performance will be expressed thereafter in the frequency domain. Since $P = 0$, we have $r_i = \sum b_{ij} u_j$, where u_j is the true location of the anchors and the performance (steady-sate error, convergence speed) is defined by the tracking performance of the dynamics, T_s. Let us define a transfer function, $S(s)$, between the reference input, r_i, and tracking error, defined as $\varepsilon_i^{ref} \triangleq x_i^* - x_i$, which for $K = \alpha$ is

$$S(s) = (1 + K(s)\tfrac{1}{s})^{-1} = s(s+\alpha)^{-1}. \tag{10}$$

For all $\alpha > 0$, $S(s)$ is stable with a zero at the origin implying 0 steady-state error for constant inputs. It is important to note that the cutoff frequency, ω_S, for which $|S(j\omega_S)| = \frac{\sqrt{2}}{2}$, is $\omega_S = \alpha$. The magnitude of S is close to zero in the Low Frequency (LF) range ($\omega \ll \omega_S$) and approaches 1 in the High Frequency (HF) range ($\omega \gg \omega_S$). Increasing α increases the cutoff frequency of S implying an increase in the convergence speed, which follows Theorem 1.

To proceed with the subsequent analysis, note that

$$\begin{aligned} T_{z_i \to x_i}(s) &= T_{r_i \to x_i}(s) = \tfrac{\alpha}{s+\alpha} = 1 - S(s) \triangleq T(s), \\ T_{z_i \to y_i}(s) &= T_{r_i \to y_i}(s) = \tfrac{\alpha s}{s+\alpha} = K(s)S(s) \triangleq KS(s). \end{aligned} \tag{11}$$

The cutoff frequency, ω_T, of $T(s)$ is equal to the cutoff frequency, ω_S, of $S(s)$. Increasing α increases both ω_T and ω_S, and thus the bandwidth of $T(s)$. Since the magnitude of $T(s)$ is equal to 1 in the LF range and decreases in the HF range, increasing α implies the transmission of a broader frequency range of disturbance, z_i, on the output, x_i. It is therefore not possible to increase the convergence speed and disturbance rejection at the same time. This is also true for the dynamic controller, $K(s)$; we may, however, impose a larger slope of magnitude decay in $T(s)$. Let us now consider the transfer function, $KS(s)$. In the HF range, $|KS(s)| = \alpha$, and thus an increase in α amplifies the disturbance. A logical extension is to consider a dynamic controller, $K(s)$, which is frequency-dependent such that it has a high gain in the LF range, for a good tracking performance; and a low gain in the HF range for a better disturbance rejection.

B. Rejection vs. Localization tradeoff, $M > 1$

To study the general case, let us define the global transfer function, $\tilde{S}^g_{u \to \varepsilon^{ref}}$, as an $M \times N$ matrix between the input, u (anchors positions), and the network tracking error, defined by $\varepsilon^{ref} \triangleq x^* - x$. Note that we can write the input as $u = \frac{u}{\|u\|}\|u\|$, where $\|u\|$ is the Euclidean norm of u. In this case, the tracking performance of the network could be evaluated by the $M \times 1$ transfer function:

$$S^g_{\|u\| \to \varepsilon^{ref}} = \tilde{S}^g_{u \to \varepsilon^{ref}} \frac{u}{\|u\|} \triangleq S^g, \tag{12}$$

whose j-th component, S^g_j, is the transfer function between the constant, $\|u\|$, and j-th sensor's tracking error, ε_j^{ref}. Let us define additional global transfer functions as follows:

$$T_{z \to x}(s) \triangleq T^g(s), \qquad T_{z \to y}(s) \triangleq KS^g(s). \tag{13}$$

The transfer functions T^g and KS^g are $M \times M$ matrices, components of which, T^g_{ij} and KS^g_{ij}, represent transfer functions between j-th sensor disturbance, z_j, and i-th sensor location estimate, x_i, and control signals, y_i, respectively.

In general, the components of S^g, T^g, and KS^g are different form the local dynamics, S, T, and KS. However, increasing α has the same consequences as discussed before in the simple case. We illustrate this numerically[2] in Fig. 4, which shows the maximal singular value, $\bar{\sigma}(\cdot)$, of frequency responses of S^g, T^g, and KS^g for a network of $M = 20$ sensors with $P \neq 0$ and for α varying form 1 to 10^4. Briefly, $\bar{\sigma}(\cdot)$ is a generalization of gain for MIMO systems, [32], and its maximum value for a given frequency is the maximum amplification between the Euclidean norms of input-output vectors (over all directions of applied input vector). We observe that similar to the local case, $M = 1$, an increase of α increases the convergence speed but also increases HF disturbance amplification.

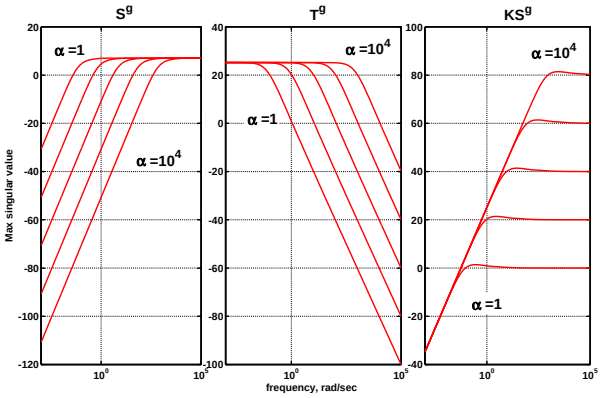

Fig. 4. Maximal singular value of S^g, T^g, and KS^g vs. α

As in the case with $M = 1$, in order to reduce the HF disturbance amplification, it is possible to use a dynamic controller, $K(s)$, that decreases the maximum HF singular value of T^g and KS^g. However, the design of such controller in the general case of $M > 1$ is a non-trivial problem and could result in poor performance (low speed, high oscillations) and a global system instability for some choice of $K(s)$. In fact, it is a special case of the decentralized control problem, which is proved to be NP-hard even in the LTI case, [33]. However, since the sensors are identical it is possible to link the global network to the local dynamics and then perform a local design by the traditional H_∞ approach. This method is proposed in [26], [27] and is applied, with some changes, to DILOC-CT in the next section.

[2]It is possible to compute the closed-form expressions of S^g, T^g, and KS^g, e.g., by using the Lower Fractional Transformation algebra (LFT), [31], but this computation is beyond the scope of this paper.

IV. DILOC-CT: H_∞ DESIGN

We now consider DILOC-CT introduced earlier in Section II-B with local controllers. We assume that the barycentric matrices, P and B, are given[3]. Our objective is to design identical (local) controllers, $K(s)$, to achieve, besides the global system stability, certain performance objectives, summarized in Table I. We note that the location estimator at each sensor is identical and define the following global system description for each coordinate, recall Eq. (11):

$$x = (I_M \otimes T(s))\, r^z, \tag{14}$$

where $r^z = r + z = Px + B_u u_0 + z$, and $u_0 = \|u\|, B_u = B\frac{u}{u_0}$. Next note that $\varepsilon^{ref} = x^* - x = (I_M - P)^{-1} B_u u_0 - x$, and $\varepsilon = r^z - x$, from Fig. 3. We have the following relation:

$$\begin{bmatrix} r^z \\ \varepsilon^{ref} \\ \varepsilon \end{bmatrix} = \underbrace{\left[\begin{array}{c|cc} P & B_u & I_M \\ \hline -I_M & (I_M - P)^{-1} & 0 \\ P - I_M & B_u & I_M \end{array}\right]}_{H} \begin{bmatrix} x \\ u_0 \\ z \end{bmatrix}. \tag{15}$$

The local transfer function, $T(s)$, identical at each sensor, is

$$T(s) = \frac{K(s)\frac{1}{s}}{1 + K(s)\frac{1}{s}} \tag{16}$$

Given the representation in Eqs. (14) and (15), we have

$$T_{\left[\begin{smallmatrix} u_0 \\ z \end{smallmatrix}\right] \to \left[\begin{smallmatrix} \varepsilon^{ref} \\ \varepsilon \end{smallmatrix}\right]} = (I_M \otimes T(s)) \star H, \tag{17}$$

and $T_{u_0 \to \varepsilon^{ref}}(s) = S^g(s)$, see Eq. (12). Furthermore, $T^g(s)$ and $KS^g(s)$ can be written in terms of $T_{z\to\varepsilon}(s)$ as

$$T^g(s) = \frac{K(s)}{s} T_{z\to\varepsilon}(s), \quad KS^g(s) = K(s) T_{z\to\varepsilon}(s). \tag{18}$$

We formulate the following control design problem:

Problem 1 (Control problem): Given the global system in Eqs. (14) and (15), find the local controller, $K(s)$, such that the global system is stable and satisfies the following frequency constraints:

$$\begin{array}{ll} \overline{\sigma}\left(S^g(j\omega)\right) \le \Omega_S(\omega), & \text{in LF range,} \\ \overline{\sigma}\left(T^g(j\omega)\right) \le \Omega_T(\omega), & \text{in HF range,} \\ \overline{\sigma}\left(KS^g(j\omega)\right) \le \Omega_{KS}(\omega), & \text{in HF range.} \end{array} \tag{19}$$

We now briefly explain the frequency constraints. The first constraint, Ω_S, ensures zero steady-state error and provides a handle on the speed of convergence. The second constraint, Ω_T, imposes a maximum bandwidth on T^g, which, in turn, limits the disturbance amplification in high-frequency. The last constraint, Ω_{KS}, reduces the amplification of noise on the local input, y, to each sensor's local dynamics in high-frequency. Specifics on these constraints are tabulated in Table I and are further elaborated in Section V.

[3]Note that the controller design requires the knowledge of all barycentric coordinates, P and B, which may be restrictive. However, we stress that the resulting controller is local and the procedure described here is critical to any future work on decentralized design. In addition, computing the locations at a central location from the matrices, P and B, and then transmitting them to the sensors incurs noise in the communication that is not suppressed; this procedure is further susceptible to cyber attacks revealing the sensor locations to an adversary.

TABLE I
DILOC-CT DESIGN SPECIFICATIONS

Performance specs.	Frequency constraint	Range
Zero steady-state	Slope of $+20$ dB/dec for $\overline{\sigma}\left(S^g(j\omega)\right)$	LF
Conv. speed	Cutoff freq. of $\overline{\sigma}(S^g) \ge 10$ rad/sec	LF
Disturbance reduction	-60 dB/dec slope for $\overline{\sigma}\left(T^g(j\omega)\right)$	HF
	-40 dB/dec slope for $\overline{\sigma}\left(KS^g(j\omega)\right)$	HF

In order to solve the above control problem, we will use the well-known input-output approach, which was introduced to deal with interconnected systems, see [24]–[27] for details.

A. Input-output Approach

We now describe the input-output approach over which we will formulate the DILOC-CT controller design problem. We use the concept of dissipitavity taken from [24]–[27], a simplified version of which is defined below.

Definition 1 (Dissipativity): An LTI, stable, and causal operator, H, is *strictly* $\{X, Y, Z\}$*-dissipative*, where $X = X^T, Y, Z = Z^T$, are real matrices such that

$$\begin{bmatrix} X & Y \\ Y^T & Z \end{bmatrix}$$

is full-rank; if $\exists\ \varepsilon > 0$ such that for almost all $\omega > 0$

$$\begin{bmatrix} I \\ H(j\omega) \end{bmatrix}^* \begin{bmatrix} X & Y \\ Y^T & Z \end{bmatrix} \begin{bmatrix} I \\ H(j\omega) \end{bmatrix} \le -\varepsilon I. \tag{20}$$

If the inequality in Eq. (20) is satisfied with $\varepsilon = 0$, the operator is said to be $\{X, Y, Z\}$*-dissipative*.

Consider a large-scale system represented as an interconnection, $\widetilde{H}$, of identical subsystems, T_s:

$$p = (I \otimes T_s)(q), \qquad \begin{bmatrix} q \\ \widetilde{z} \end{bmatrix} = \widetilde{H}\left(\begin{bmatrix} p \\ \widetilde{w} \end{bmatrix}\right), \tag{21}$$

where

$$\widetilde{H} = \begin{bmatrix} \widetilde{H}_{11} & \widetilde{H}_{12} \\ \widetilde{H}_{21} & \widetilde{H}_{22} \end{bmatrix}$$

is a finite-dimensional, stable LTI system, $T_s = G \star K$, $\widetilde{w}(t)$ is the input vector, $\widetilde{z}(t)$ is the output vector, and $q(t), p(t)$, are internal signals. The LTI systems, G and K, are finite-dimensional and are referred to as the local plant and controller. The global transfer function between external input, $\widetilde{w}$, and output, $\widetilde{z}$, is

$$T_{\widetilde{w}\to\widetilde{z}} = (I \otimes T_s) \star \widetilde{H},$$

and its H_∞ norm is ensured by the local controller, K, by the following theorem.

Theorem 2: Given $\eta > 0$, a stable LTI system, $\widetilde{H}$, a local plant, G, and real matrices, $X = X^T \ge 0$, Y, $Z = Z^T$, *if there exist*

(i) a positive-definite matrix, Q, such that $\widetilde{H}$ is $\{\text{diag}(Q \otimes X, -\eta^2 I), \text{diag}(Q \otimes Y, 0), \text{diag}(Q \otimes Z, I)\}$-dissipative, and
(ii) a local controller, K, such that $T_s = G \star K$ is strictly $\{-Z, -Y^T, -X\}$-dissipative,

then the local controller, K, ensures that the global system, $(I_{N_s} \otimes T_s) \star \widetilde{H}$, is stable and

$$\| (I \otimes T_s) \star \widetilde{H} \|_\infty \leq \eta. \tag{22}$$

The proof of Theorem 2 can be found in [26], [27], and it relies on a version of the graph-separation theorem used in [24] for global stability and an S-procedure, [34], for global performance. It can also be seen as a generalization of the Kalman-Yakubovich-Popov lemma, [35].

B. Local Control for Global Performance

Note that based on the properties of the H_∞ norm:

$$\begin{array}{rl} \left\| \begin{array}{cc} T_{11} & T_{12} \\ T_{21} & T_{22} \end{array} \right\|_\infty \leq \eta \Rightarrow & \begin{array}{l} \|T_{11}\|_\infty \leq \eta, \\ \|T_{22}\|_\infty \leq \eta, \end{array} \\ \Leftrightarrow \begin{array}{l} \overline{\sigma}\left(T_{11}\left(j\omega\right)\right) \leq \eta \\ \overline{\sigma}\left(T_{22}\left(j\omega\right)\right) \leq \eta \end{array} & , \forall \omega \in \mathbb{R}^+, \end{array} \tag{23}$$

Theorem 2 is applicable to the system in Eqs. (14) and (15) to find a controller, K, ensuring a global bound, η, on the H_∞ norm of, in this case, $T_{11} = S^g$ and $T_{22} = T_{z \to \varepsilon}$. However, such imposed constraints are frequency-independent. We now present a result allowing to impose frequency-dependent bounds, Eq. (19), constructed with the help of local transfer functions, KS, S, or T, and constant gains. Consider the following augmented localization system:

$$\begin{array}{rcl} \left[\begin{array}{c} \overline{x} \\ x \end{array} \right] & = & \left(I_{M+1} \otimes T(s)\right) \left[\begin{array}{c} \overline{r} \\ r \end{array} \right], \\ \left[\begin{array}{c} \overline{r} \\ r \\ \overline{\varepsilon}^{ref} \\ \overline{\varepsilon} \end{array} \right] & = & \underbrace{\left[\begin{array}{cccc} l & 0 & g_1 l & 0 \\ l B_u & P & g_1 l B_u & g_3 I \\ g_1^{-1} l \overline{P} & -g_1^{-1} I & l \overline{P} & 0 \\ g_2 l B_u & g_2 (P - I_M) & g_2 g_1 l B_u & g_2 g_3 I \end{array} \right]}_{\overline{H}} \left[\begin{array}{c} \overline{x} \\ x \\ \overline{u} \\ \overline{z} \end{array} \right], \end{array} \tag{24}$$

with real positive scalars, g_1, g_2, g_3, $l = \frac{1}{1+\beta}$, $0 < \beta \ll 1$, $\overline{P} = \left(I_M - P\right)^{-1} B_u$, and one additional local sensor dynamics, $T(s)$, with additional input, $\overline{r}$, and output, $\overline{x}$.

The main result of this paper is now provided in the following theorem that solves Problem 1 following a similar argument as in Section IV-A.

Theorem 3 (Control Design): Given $\eta > 0$, the system described in Eq. (24), and real scalars, $X \geq 0, Y, Z \leq 0$, *if there exists* a positive-definite matrix, $Q \in \mathbb{R}^{(M+1)\times(M+1)}$, such that

(i) $\overline{H}$ is $\left\{\text{diag}\left(XQ, -\eta^2 I\right), \quad \text{diag}\left(YQ, 0\right), \quad \text{diag}\left(ZQ, I\right)\right\}$-dissipative,

and a local controller, K, such that:

(ii) $T(s)$ is strictly $\{-Z, -Y, -X\}$-dissipative with $\|\hat{T}(s)\|_\infty < 1$, and $\hat{T}(s) = \left(T(s) + \frac{Y}{X}\right) \sqrt{\frac{X^2}{Y^2 - XZ}}$;

(iii) $|S\left(j\omega\right)| \leq \eta^{-1} \Omega_S\left(\omega\right)$, in the LF range;

(iv) $|KS\left(j\omega\right)| \leq \eta^{-1} g_2 g_3 \min\left\{\Omega_{KS}\left(\omega\right), \omega \Omega_T\left(\omega\right)\right\}$, in the HF range;

then the local controller K solves the Problem 1.

Proof: Let us define weighted version of input-output signals of the original system in Eq. (15) as:

$$\begin{array}{rcl} \overline{\varepsilon}^{ref} & = & g_1^{-1} \varepsilon^{ref}, \\ \overline{\varepsilon} & = & g_2 \varepsilon, \\ \overline{z} & = & g_3^{-1} z, \\ \overline{u} & = & g_1^{-1} \left(S + \beta\right) u_0. \end{array}$$

Based on this notation, one can define the following relation:

$$T_{\left[\begin{smallmatrix} \overline{u} \\ \overline{z} \end{smallmatrix}\right] \to \left[\begin{smallmatrix} \overline{\varepsilon}^{ref} \\ \overline{\varepsilon} \end{smallmatrix}\right]} = W_1 T_{\left[\begin{smallmatrix} u_0 \\ z \end{smallmatrix}\right] \to \left[\begin{smallmatrix} \varepsilon^{ref} \\ \varepsilon \end{smallmatrix}\right]} W_2,$$

with[4] $W_1 = \left[\begin{smallmatrix} g_1^{-1} & 0 \\ 0 & g_2 I_M \end{smallmatrix}\right]$ and $W_2 = \left[\begin{smallmatrix} g_1 (S(s) + \beta)^{-1} & 0 \\ 0 & g_3 I_M \end{smallmatrix}\right]$.

Since $S(s) = T(s) - 1$, the matrix transfer function, W_2, can be represented in the form of an interconnection (LFT) of one system $T(s)$:

$$W_2 = T(s) \star H^W,$$

with $H^W = \left[\begin{array}{c|cc} l & g_1 l & 0 \\ \hline l & g_1 l & 0 \\ 0 & 0 & g_3 \end{array}\right]$.

The global transfer function, Eq. (15), is an LFT of M systems, $T(s)$, and is defined by

$$T_{\left[\begin{smallmatrix} u_0 \\ z \end{smallmatrix}\right] \to \left[\begin{smallmatrix} \varepsilon^{ref} \\ \varepsilon \end{smallmatrix}\right]} = \left(T(s) I_M\right) \star H.$$

The augmented system, $T_{\left[\begin{smallmatrix} \overline{u} \\ \overline{z} \end{smallmatrix}\right] \to \left[\begin{smallmatrix} \overline{\varepsilon}^{ref} \\ \overline{\varepsilon} \end{smallmatrix}\right]} = \left(I_{M+1} \otimes T(s)\right) \star \overline{H}$, is an LFT of $M+1$ systems, $\overline{T}(s)$, representing a series connection of $W_1 T_{\left[\begin{smallmatrix} u_0 \\ z \end{smallmatrix}\right] \to \left[\begin{smallmatrix} \varepsilon^{ref} \\ \varepsilon \end{smallmatrix}\right]}$ and W_2, and is given in Eq. (24). The corresponding expression of $\overline{H}$ is computed based on the LFT algebra, see Section 2.4 in [31], .

Note that the first two conditions of Theorem 3 correspond to the two conditions of Theorem 2. Applying Theorem 2, a controller that ensures second condition of Theorem 3, therefore, ensures the global transfer function bound:

$$\left\| \left(T(s) I_{M+1}\right) \star \overline{H} \right\|_\infty = \left\| W_1 T_{\left[\begin{smallmatrix} u_0 \\ z \end{smallmatrix}\right] \to \left[\begin{smallmatrix} \varepsilon^{ref} \\ \varepsilon \end{smallmatrix}\right]} W_2 \right\|_\infty \leq \eta.$$

Using Eq. (23), the last inequality implies $\forall \omega$:

$$\begin{array}{rcl} \overline{\sigma}\left(T_{u_0 \to \varepsilon^{ref}}\left(j\omega\right)\right) & \leq & \eta \left|S\left(j\omega\right) + \beta\right|, \\ \overline{\sigma}\left(T_{z \to \varepsilon}\left(j\omega\right)\right) & \leq & \eta \left(g_2 g_3\right)^{-1}. \end{array} \tag{25}$$

For frequency range where β can be neglected compared to $|S\left(j\omega\right)|$, condition *(iii)* of the Theorem 3 ensures the first condition of Problem 1. Note that in the HF range:

$$|KS\left(j\omega\right)| = \frac{|K\left(j\omega\right)|}{\left|1 - \frac{j}{\omega} K\left(j\omega\right)\right|} \approx |K\left(j\omega\right)|.$$

Therefore, together with Eq. (18), the condition *(iv)* implies the second and third conditions of the Problem 1. ■

[4]The reason of using parameter β is that in order to properly define the H_∞ norm, the weighting filters W_i should be stable transfer functions. Since S has zero at zero, Eq. (10) (because of presence of integrator in local sensor dynamics, see Fig 3), the weighting filter W_2 would contain integrator and thus be unstable with $\beta = 0$. This is a classical problem in the H_∞ design, [32], which is practically solved by perturbing the pure integrator, $\frac{1}{s}$, by a small real parameter, $\beta : \frac{1}{s} \to \frac{1}{s+\beta}$.

Remark 1: Theorem 3 can be applied to efficiently design a controller, K, that solves Problem 1, if X, Y, and Z, are fixed. In this case, the first condition of Theorem 3 is a Linear Matrix Inequality (LMI) with respect to the decision variables, η and Q, and thus, convex optimization can be applied to find the smallest η such that it is satisfied. The conditions, *(ii)-(iv)*, are ensured by the local traditional H_∞ design. However, if X, Y, and Z, are the decision variables, the underlying optimization becomes bilinear. In this case, a quasi-convex optimization problem for finding X, Y, and Z, that satisfy the condition *(i)* and relaxes the condition *(ii)* of Theorem 3 is proposed in [26], [27] and is used thereafter.

Remark 2: The weighting filters, W_1 and W_2, are used to impose frequency-dependent bounds on the global transfer function magnitudes, Eq. (19), in a relative fashion, i.e., global performance in Eq. (19) is ensured by the local system performance, see conditions *(iii)-(iv)* of Theorem 3. The reason for using different gains, g_i, is to impose the constraint on diagonal blocks, $T_{u_0 \to \varepsilon^{ref}}$ and $T_{z \to \varepsilon}$, while reducing this constraint on the cross transfer functions, $T_{u_0 \to \varepsilon}$ and $T_{z \to \varepsilon^{ref}}$, if such constraints are not needed from application point of view.

V. Numerical Examples

We consider a network of $M = 20$ sensors and $N = m + 1 = 3$ anchors in $\mathbb{R}^2$. The sensors lie in the convex hull (triangle) formed by the anchors, see Fig. 5 (Left) for a candidate deployment where the DILOC-CT trajectories, with arbitrary initial conditions marked by '$\star$', are shown for four randomly chosen sensors. Each sensor is connected to three neighbors such that it lies in their convex hull. Fig. 5 (Right) shows the normalized sum of squared error (averaged across all sensors and all dimensions) for different values of the proportional gain without disturbance, z.

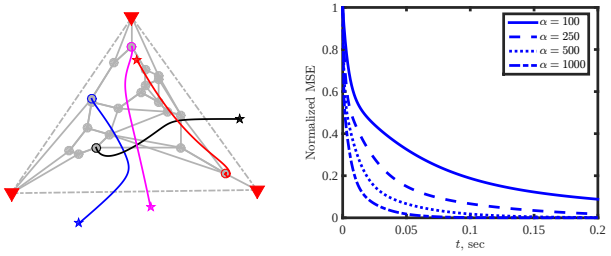

Fig. 5. DILOC-CT: Network and convergence speed

Next consider the disturbance, z, each component of which is a realization of a band-limited noise with amplitude, $A < 5$, in frequency range, $[\omega_z^- \ \omega_z^+] = [600 \ 10^5]$ rad/sec. To reduce the contribution of this noise on the location estimate, x, and the *control command*, y, i.e., the input to the integrator in the local dynamics, T_s, see Fig. 3, while ensuring the imposed tracking performance, see Table I, we add the frequency constraints, $\Omega_S(\omega), \Omega_T(\omega), \Omega_{KS}(\omega)$ in Problem 1, shown as red dotted lines in Fig. 6. We define the augmented system, Eq. (24), with $g_1 = 1$, $g_2 = 14$, $g_3 = 1.7$ and $\beta = 10^{-3}$. Using the quasi-convex optimization problem proposed in [26], [27], the sensor dissipativity characterization is defined by $X = -4.99$, $Y = 1.99$, and $Z = 1$. First condition of Theorem 3 is ensured with minimum $\eta = 48.85$ by convex LMI optimization. The local controller, $K(s)$, is then computed using standard H_∞ design [32] to ensure conditions *(ii)-(iv)* of Theorem 3:

$$K(s) = \frac{3.71 \cdot 10^9}{(s + 2094)(s + 6712)}.$$

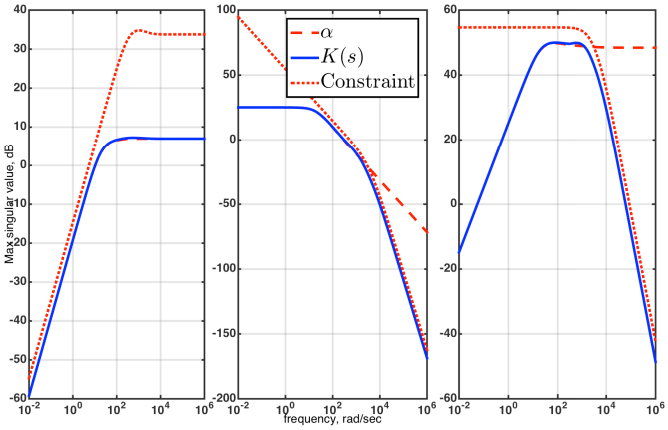

Fig. 6. Singular value of S^g, T^g and KS^g for different frequencies and for dynamic $K(s)$ (solid blue line) and static α (red dashed line) cases together with corresponding frequency constraints (red dotted line).

As expected, the local controller is a low-pass filter with high gain, $G_K \approx 264$, in the LF range, and the negative slope (-40 dB/dec) in the HF range. According to the Theorem 3, the designed controller solves the Problem 1, i.e., it ensures the frequency constraints, Eq. (19), as can be verified in Fig. 6. Furthermore, the performance of this controller is compared to the static (proportional) gain with $\alpha = 264$, which ensures the same convergence speed, see red dashed lines in Fig. 6. It is interesting to note that the LF gain of the dynamic controller is the same as with the static gain, $\alpha = 264$; however, in the HF range, the dynamic controller allows to significantly reduce the maximum singular values of T^g and KS^g, which subsequently results in disturbance reduction. All these frequency domain observations are confirmed by temporal simulations presented in Fig. 7 where mean estimation error, ε^{ref}, and command signals, y_i's, are presented for both cases.

VI. Conclusions

In this paper, we describe a continuous-time LTI algorithm, DILOC-CT, to solve the sensor localization problem in $\mathbb{R}^m$ with at least $m+1$ anchors who know their locations. Assuming that each sensor lies in the convex hull of the anchors, we show that DILOC-CT converges to the true sensor locations (when there is no disturbance) and the convergence speed can be increased arbitrarily by using a proportional gain. Since high gain results into unwanted transients, large input to each sensors internal integrator, and amplification of network-based disturbance, e.g., communication noise;

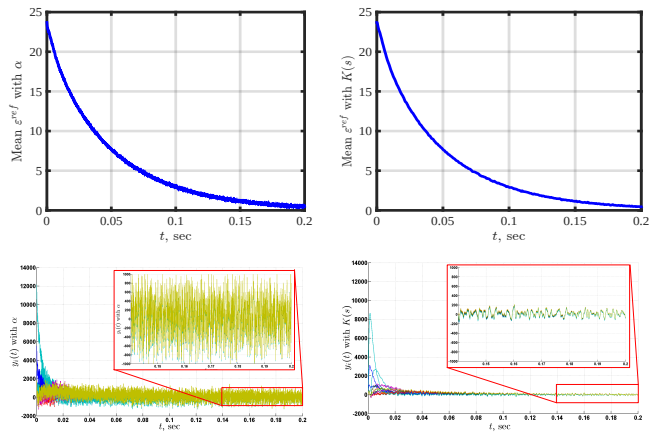

Fig. 7. Temporal simulations: (Left) Static, α; (Right): Dynamic, $K(s)$. Note the high values of the control command, $y_i(t)$'s, with the proportional controller, that could overexcite the local system, integrator, at each sensor.

we design a dynamic controller with frequency-dependent performance objectives using the H_∞ theory. We show that this dynamic controller does not only provide disturbance rejection but is also able to meet certain performance objectives embedded in frequency-dependent constraints. Finally, we note that although the design requires the knowledge of the entire barycentric matrices, the approach described in this paper serves as the foundation of future investigation towards decentralized design of dynamic controllers.

REFERENCES

[1] G. Destino, *Positioning in Wireless Networks: Non-cooperative and Cooperative Algorithms*, Ph.D., University of Oulu, 2012.

[2] R. L. Moses, D. Krishnamurthy, and R. Patterson, "A self-localization method for wireless sensor networks," *EURASIP Journal on Applied Signal Processing*, , no. 4, pp. 348–358, Mar. 2003.

[3] N. Patwari, A. O. Hero III, M. Perkins, N. Correal, and R. J. ODea, "Relative location estimation in wireless sensor networks," *IEEE Trans. on Signal Processing*, vol. 51, no. 8, pp. 2137–2148, Aug. 2003.

[4] Y. Shang, W. Ruml, Y. Zhang, and M. Fromherz, "Localization from mere connectivity," in *4th ACM international symposium on mobile ad-hoc networking and computing*, Annapolis, MD, Jun. 2003, pp. 201–212.

[5] Y. Shang and W. Ruml, "Improved MDS-based localization," in *IEEE Infocom*, Hong Kong, Mar. 2004, pp. 2640–2651.

[6] M. Cao, B. D. O. Anderson, and A. S. Morse, "Localization with imprecise distance information in sensor networks," in *44th IEEE Conference on Decision and Control*, Sevilla, Spain, Dec. 2005, pp. 2829–2834.

[7] N. Patwari and A. O. Hero III, "Manifold learning algorithms for localization in wireless sensor networks," in *IEEE ICASSP*, Montreal, Canada, Mar. 2004, pp. 857–860.

[8] A. Beck, P. Stoica, and J. Li, "Exact and approximate solutions of source localization problems," *IEEE Transactions on Signal Processing*, vol. 56, no. 5, pp. 1770–1778, May 2008.

[9] B. D. O. Anderson, I. Shames, G. Mao, and B. Fidan, "Formal theory of noisy sensor network localization," *SIAM Journal of Discrete Mathematics*, vol. 24, no. 2, pp. 684–698, 2010.

[10] P. Biswas, T.-C. Lian, T.C. Wang, and Y. Ye, "Semidefinite programming based algorithms for sensor network localization," *ACM Transactions on Sensor Networks*, vol. 2, no. 2, pp. 188–220, May 2006.

[11] Y. Ding, N. Krislock, J. Qian, and Henry Wolkowicz, "Sensor network localization, Euclidean distance matrix completions, and graph realization," *Optimization and Engineering*, vol. 11, no. 1, pp. 45–66, 2010.

[12] I. Shames, P. T. Bibalan, B. Fidan, and B. D. O. Anderson, "Polynomial methods in noisy network localization," in *17th Mediterranean Conference on Control and Automation*, Jun. 2009, pp. 1307–1312.

[13] A. Savvides, H. Park, and M. B. Srivastava, "The bits and flops of the n-hop multilateration primitive for node localization problems," in *Intl. Workshop on Sensor Networks and Applications*, Atlanta, GA, Sep. 2002, pp. 112–121.

[14] R. Nagpal, H. Shrobe, and J. Bachrach, "Organizing a global coordinate system from local information on an ad-hoc sensor network," in *2nd Intl. Workshop on Information Processing in Sensor Networks*, Palo Alto, CA, Apr. 2003, pp. 333–348.

[15] J. A. Costa, N. Patwari, and A. O. Hero III, "Distributed weighted-multidimensional scaling for node localization in sensor networks," *ACM Transactions on Sensor Networks*, vol. 2, no. 1, pp. 39–64, 2006.

[16] J. Albowicz, A. Chen, and L. Zhang, "Recursive position estimation in sensor networks," in *IEEE Int. Conf. on Network Protocols*, Riverside, CA, Nov. 2001, pp. 35–41.

[17] S. Čapkun, M. Hamdi, and J. P. Hubaux, "GPS-free positioning in mobile ad-hoc networks," in *34th IEEE Hawaii International Conference on System Sciences*, Wailea Maui, HI, Jan. 2001, pp. 1–10.

[18] J. Fang, M. Cao, A. S. Morse, and B. D. O. Anderson, "Sequential localization of sensor networks," *SIAM Journal on Control and Optimization*, vol. 48, no. 1, pp. 321–350, 2009.

[19] M. Deghat, I. Shames, B. D. O. Anderson, and J. M. F. Moura, "Distributed localization via barycentric coordinates: Finite-time convergence," in *18th IFAC World congress*, Milano, Italy, Aug. 2011, pp. 7824–7829.

[20] A. T. Ihler, J. W. Fisher III, R. L. Moses, and A. S. Willsky, "Nonparametric belief propagation for self-calibration in sensor networks," in *IEEE ICASSP*, Montreal, Canada, May 2004.

[21] S. Thrun, "Probabilistic robotics," *Communications of the ACM*, vol. 45, no. 3, pp. 52–57, Mar. 2002.

[22] U. A. Khan, S. Kar, and J. M. F. Moura, "Distributed sensor localization in random environments using minimal number of anchor nodes," *IEEE Transactions on Signal Processing*, vol. 57, no. 5, pp. 2000–2016, May 2009.

[23] August Ferdinand Möbius, *Der barycentrische calcul*, 1827.

[24] P. J. Moylan and D. J. Hill, "Stability criteria for large-scale systems," *IEEE Trans. Aut. Control*, vol. AC-23, no. 2, pp. 143–149, Apr. 1978.

[25] G. Scorletti and G. Duc, "An LMI approach to decentralized H_∞ control," *Int. J. Control*, vol. 74, no. 3, pp. 211–224, 2001.

[26] A. Korniienko, G. Scorletti, E. Colinet, and E. Blanco, "Control law design for distributed multi-agent systems," Tech. Rep., Laboratoire Ampère, Ecole Centrale de Lyon, 2011.

[27] A. Korniienko, G. Scorletti, E. Colinet, and E. Blanco, "Performance control for interconnection of identical systems: Application to pll network design," *International Journal of Robust and Nonlinear Control*, Dec. 2014.

[28] Yoon-Gu Kim, Jinung An, and Ki-Dong Lee, "Localization of mobile robot based on fusion of artificial landmark and RF TDOA distance under indoor sensor network," *International Journal of Advanced Robotic Systems*, vol. 8, no. 4, pp. 203–211, September 2011.

[29] Manfred J Sippl and Harold A Scheraga, "Cayley-menger coordinates," *Proceedings of the National Academy of Sciences*, vol. 83, no. 8, pp. 2283–2287, 1986.

[30] Usman A Khan, Soummya Kar, Bruno Sinopoli, and José MF Moura, "Distributed sensor localization in euclidean spaces: Dynamic environments," in *Communication, Control, and Computing, 2008 46th Annual Allerton Conference on*. IEEE, 2008, pp. 361–366.

[31] J. Doyle, A. Packard, and K. Zhou, "Review of LFT's, LMI's and μ," in *IEEE Conf. Decision and Control*, IEEE, Ed., Brighton, England, Dec. 1991, vol. 2, pp. 1227–1232.

[32] S. Skogestad and I. Postlethwaite, *Multivariable Feedback Control, Analysis and Design*, John Wiley and Sons Chischester, 2005.

[33] V. Blondel and J. N. Tsitsiklis, "NP-hardness of some linear control design problems," *SIAM J. of Control and Opt.*, vol. 35, no. 6, 1997.

[34] V. A. Yakubovich, "The $\mathcal{S}$-procedure in non-linear control theory," *Vestnik Leningrad Univ. Math.*, vol. 4, pp. 73–93, 1977, In Russian, 1971.

[35] A. Rantzer, "On the Kalman-Yakubovich-Popov lemma," *Systems and Control Letters*, vol. 27, no. 5, Jan. 1996.